CHAPTER VI
POLYANILINE NANOPARTICLES WITH CONTROLLED SIZES USING A CROSS-LINKED CARBOXYMETHYL CHITIN TEMPLATE

6.1 Abstract

PANI nanoparticles were chemically synthesized in the presence of a cross-linked carboxymethyl chitin (CM-chitin), acting as a template. The reaction was performed under acidic conditions and the template was removed after the polymerization of aniline was completed. The morphology of the synthesized PANI was globular with a diameter in the nanometer range. The degree of cross-linking of the CM-chitin played an important role in determining the size of the obtained PANI nanoparticles, which decreased from approximately 392 nm to 160 nm with increase in concentration of the cross-linking agent, glutaraldehyde, from 0 to 9 μmole, respectively. At higher glutaraldehyde concentration (18 μmole), an aggregated PANI network was observed due to the incomplete removal of the more highly cross-linked CM-chitin. Molecular characterization (including UV-Visible, FTIR, TGA, and XRD techniques) revealed that the structure of the synthesized PANI nanoparticles is identical to that of conventional PANI. A mechanism is proposed for the formation of PANI nanoparticles in the presence of the cross-linked CM-chitin template.

6.2 Introduction

Polyaniline, as a conductive polymer, has attracted particular attention because of its unique electronic properties, ease of synthesis, environmental stability, and low cost of the monomer (Bai *et al.* 2007; Li, Gou *et al.* 2006; Li, Zhoa *et al.* 2007; Zhang and Wan 2006), as well as its potential applications in many areas including sensors, actuators, batteries, and anticorrosion coatings (Cho *et al.* 2004; Thanpitcha *et al.* 2006). In recent years, much attention has been given to the synthesis of PANI nanostructures such as nanorods (Stejskal *et al.* 2006; Wei *et al.* 2006), nanofibers (Chiou and Epstein 2005; Wang, Jing, and Kong 2007), and

nanospheres (Cheng, Ng, and Chan 2005; Zhu and Jiang 2007) with the expectation that such species may show superior properties to conventionally-polymerized materials (Cheng, Jiang *et al.* 2004; He, 2005; Xing *et al.* 2006). For example, one might expect enhanced responsiveness for sensor applications (Huang, Virji *et al.* 2004; Virji *et al.* 2004), improved dispersion (Hopkins *et al.* 2004) and a lower percolation threshold for electrical conductivity for PANI nanoparticles in composite materials (Banerjee and Mandal 1995).

The synthesis of PANI nanostructures has been achieved by either the chemical or electrochemical polymerization of aniline with the aid of a hard template, such as a zeolite channel (Cao *et al.* 1992; Wu and Bein 1994), track-etched polycarbonate (Liu and Kaner 2004; Martin 1996), or anodized alumina (Wang, Chen, and Li 2002; Xiong, Wang, and Xia 2004), or a soft template, such as a surfactant (Xiong, Wang, and Xia 2004; Yang et al. 2005), or polyelectrolyte (Lu *et al.* 2005). Moreover, physical methods such as electrospinning (Li, Gou *et al.* 2006), mechanical stretching (Gu *et al.* 2005; He, Li, and Tao 2001), interfacial polymerization (He 2005; Huang and Kaner 2004), rapid mixing polymerization (Wang and Jing 2008), sonochemical synthesis (Jing *et al.* 2006; 2007), radiolytic synthesis (Wang and Jing 2005), and photolithographic synthesis (Werake *et al.* 2005), and seeded polymerization (Zhang, Goux, and Manohar 2004) have been utilized in the synthesis of PANI nanostructures. Among these methods, the use of hard templates has been shown to offer an effective approach for controlling morphology, size, and size distribution of the PANI nanostructures (Mazur *et al.* 2003; Zhang and Wang 2006). Typically, the pores of the hard template can be viewed as nanoreactors, in which nanoparticles of the desired material are synthesized, whose shapes and sizes depend only on the pore topology and pore size (Xiong, Wang, and Xia 2004). However, the disadvantages of this method are, first, a rather tedious post-synthesis treatment is required to remove the template (Zhang and Wan 2002), and, second, the synthesized PANI nanostructures may be destroyed or form undesirable aggregated structures after release from the template (Zhang and Wan 2006). Therefore, the search for other approaches, which can diminish the drawbacks of the hard template, while retaining the ability to control the morphology,

size, and size distribution of the synthesized PANI nanostructures remains a challenge.

Hydrogels are three-dimensional network structures, obtained by physically or chemically cross-linking hydrophilic polymers. Due to the ability to absorb a large amount of water into the individual pores in their networks, each pore of the hydrogel can function as a single nanoreactor or a template to sequester the monomers for subsequent polymerization. Mohan *et al.* (2007) used a hydrogel network as a template, to prepare well-defined and uniform silver nanoparticles. They found that the size of the silver nanoparticles decreased with increase in the degree of cross-linking of the hydrogel (Mohan *et al.* 2007). This implies that, by increasing the degree of cross-linking of the hydrogel, smaller pore sizes are obtained, resulting in a more limited space for monomer accumulation (Strachotova *et al.* 2007). Thus, control of the size of the synthesized nanostructures may be achieved by controlling the degree of cross-linking of the hydrogel template.

Carboxymethyl chitin (CM-chitin) is an anionic water-soluble derivative of chitin obtained by the carboxymethylation reaction of chitin powder with monochloroacetic acid under basic condition. Additionally, solutions of CM-chitin can be cross-linked with glutaraldehyde to form hydrogels. This suggests the possibility that such hydrogels can serve as the reaction template for the synthesis of PANI nanostructures.

In the present work, we report a simple process to synthesize PANI nanoparticles with controllable sizes, and with narrow size distribution, by using cross-linked CM-chitin as the hydrogel template. A mechanism for the formation of PANI nanoparticles in cross-linked CM-chitin hydrogels is proposed, and the effect of glutaraldehyde concentration, used as the cross-linking agent, on the size of the PANI nanoparticles is explored.

6.3 Experimental

6.3.1 Materials

The aniline monomer, purchased from Merck, was distilled under reduced pressure prior to use. AR grade ammoniumperoxodisulfate (APS) was also purchased from Merck.

Chitin, with a degree of deacetylation (%DD) equal to 20%, measured by the method of Baxter *et al.* (Baxter et al. 1992), was prepared from shrimp shell (*Penaeus merguiensis*), kindly supplied by Surapon Food Co. Ltd, Thailand. AR grade hydrochloric acid, sodium hydroxide, monochloroacetic acid, glutaraldehyde, ethanol, and acetone were purchased from Labscan and used as received.

6.3.2 Preparation of Carboxymethyl Chitin (CM-chitin)

CM-chitin, with a degree of substitution (DS) equal to 0.43, was prepared by the reaction of chitin powder with monochloroacetic acid under basic conditions, according to the method described by Wongpanit *et al.* (Wongpanit *et al.* 2005). In a typical procedure, CM–chitin was prepared by suspending 5 g of chitin powder in 100 g of 42 %w/w NaOH. The suspension was stored under reduced pressure for 30 min. Then, 160 g of crushed ice was added to the suspension and the mixture was stirred at below 5°C for 30 min. A pre-cooled solution at a temperature below 5°C, containing 27 g monochloroacetic acid in 70 ml of 14% w/w NaOH, was slowly added to the mixture with vigorous stirring. The reaction was maintained at 0-5°C for 30 min. After settling at room temperature overnight, the mixture was neutralized with glacial acetic acid, and subsequently dialyzed in running water, followed by dialysis with distilled water for 1 day. The dialysate was centrifuged at 10,000 rpm for 10 min to remove insoluble material. A white solid was recovered from the supernatant by adding it drop-wise into acetone. The product was washed with ethanol, filtered, and dried in a vacuum at room temperature.

6.3.3 Synthesis of Polyaniline Nanoparticles

PANI nanoparticles were synthesized in aqueous solution by the oxidative polymerization of aniline using APS as an oxidizing agent, in the presence

of the cross-linked CM-chitin acting as a hydrogel template. The synthesis procedure is described as follows: CM-chitin powder (0.5 g) was added to each of four solutions of glutaraldehyde, prepared by dissolving various amounts of glutaraldehyde (0 μmole, 3 μmole, 9 μmole, 18 μmole) in 49.5 g of distilled water, in order to achieve 1 wt% of distinct glutaraldehyde-added CM-chitin solution. The mixtures were magnetically stirred overnight to complete the dissolution and cross-linking reaction of CM-chitin. 8 g of aniline (0.086 mole) was then poured into the CM-chitin solution and the mixture was cooled to 0°C with mechanical stirring at 300 rpm for 1 h. Next, 100 ml of 1.5 M HCl was added drop-wise into the suspension in a period of 30 min and the suspension was maintained with mechanical stirring for 30 min. A pre-cooled solution, at a temperature below 5°C, containing 10 g $NH_4S_2O_8$ (0.048 mole) in 100 ml of 1.5 M HCl, was added drop-wise within 30 min and the suspension was stirred at 0°C for 4 h to complete the polymerization. The resulting suspension was centrifuged at 11,000 rpm for 20 min and the precipitate was subjected to dialysis with an excess amount of distilled water until becoming neutral. The precipitated product was filtered, washed with distilled water to remove the cross-linked CM-chitin template, dried under reduced pressure for 2 days, and kept in desiccators prior to use.

6.3.4 Characterization

UV-visible spectra were obtained from a Shimadzu UV-VIS spectrometer (model 2550) in the wavelength range 250-900 nm. Aqueous 1.5 M HCl and *N*-methyl-2-pyrrolidone (NMP) were used as solvents to prepare, respectively, the emeraldine salt form (doped state) of PANI (PANI ES) and the emeraldine base form (undoped state) (PANI EB) at a concentration of 0.3 g/l.

FTIR spectra were recorded using a Thermo Nicolet Nexus 670 FTIR spectrometer in the absorbance mode at 32 scans with a resolution of 4 cm^{-1}. The spectra in the frequency range 4000-400 cm^{-1} were measured using a deuterated triglycerine sulfate detector (DTGS) with specific detectivity of 1 x 10^9 $cm \cdot Hz^{1/2} \cdot w^{-1}$.

The morphologies of the polyaniline nanoparticles were investigated using a scanning electron microscope (JOEL, model JSM-5800LV) at 15 kV. The polyaniline sample was prepared by the dispersion of the synthesized polyaniline

powder in distilled water, pipetting on to a brass stub, and drying before gold sputtering.

Thermogravimetric analysis was performed using a DuPont Instrument TGA 5.1 (model 2950) in the temperature range of 30-800°C at a heating rate of 10°C/min under a nitrogen atmosphere.

X-ray diffraction (using a Rigaku, model D/MAX-2000) was carried out in continuous mode with a scan speed of 5°/min, covering angles 2θ between 5 and 50°. Cu $K\alpha_1$ was used as the X-ray source.

The electrical conductivity was measured at 25°C using a custom-made two-point probe with an electrometer/ high resistance meter (Keithley, model 7517A).

6.4 Results and Discussion

6.4.1 UV-visible Spectra

The electronic states of the synthesized PANI nanoparticles in both emeraldine salt (PANI ES) and emeraldine base (PANI EB) forms were investigated by UV-visible spectroscopy, as shown in figure 6.1. Since dedoping may occur in NMP, a weakly basic solvent, a dispersion of the synthesized PANI in 1.5 M HCl was used to ensure a PANI ES sample. Characteristic absorption peaks were observed (Fig. 6.1a) for the synthesized PANI in 1.5 M HCl at approximately 410 and 810 nm, corresponding, respectively, to the presence of cation radicals (polarons) and the formation of bipolarons (Xian *et al.*, 2007). This confirms the doped state of PANI (PANI ES). In contrast, the PANI EB form was obtained after treating the synthesized PANI product with 0.5 M NaOH and the part of the resulting PANI soluble in NMP was used as a sample. A change characteristic of the electronic state of PANI EB was observed as a shift of the absorption peaks to 320 and 620 nm (Fig. 6.1b), assigned, respectively, to the π-π^* transition of the benzenoid ring and the exciton absorption of the quinoid ring (He 2005).

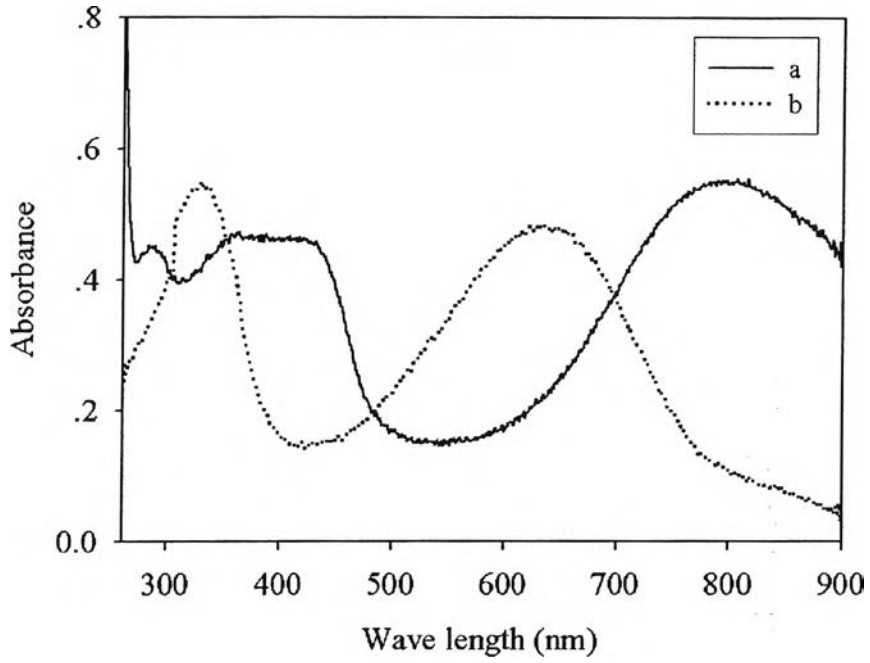

Figure 6.1 UV-visible spectra of the synthesized PANI nanoparticles: a) emeraldine salt form (PANI ES) and b) emeraldine base form (PANI EB).

6.4.2 Morphology and Possible Mechanism

The morphology of conventional PANI particles (synthesized without the addition of the CM-chitin template) as well as PANI particles synthesized in the presence of non-cross-linked CM-chitin (PANI-(1CMCT-0Glu)), as well as gluteraldehyde-cross-linked CM-chitin containing three levels of crosslinker, 3 μmole (PANI-(1CMCT-3Glu)), 9 μmole (PANI-(1CMCT-9Glu)), and 18 μmole (PANI-(1CMCT-18Glu)), were investigated by scanning electron microscopy (SEM), as shown in figure 6.2. The morphology of the conventional PANI consists of irregularly-shaped PANI aggregates (Fig. 6.2a). In contrast, the addition of 1 wt% non-cross-linked CM-chitin solution (1CMCT-0Glu) into the reaction medium caused a change in the morphology of the synthesized PANI from large, irregularly-shaped PANI aggregates to particles with relatively uniform globular shapes, having an average diameter of 392 ± 34 nm, whose surfaces are covered with radially aligned PANI dendrites, as seen in figure 6.2b. Such a change in morphology strongly suggests a formation mechanism involving self-assembly between the non-

cross-linked CM-chitin, acting as a template, and the aniline monomer. We note that such self-assembly is occurring under acidic conditions (1.5 M HCl) in which we expect protonation of the high-polarity sodium carboxymethylate groups (-$OCH_2COO^-Na^+$) to the lower polarity acid form (-OCH_2COOH) and, in contrast, the lower-polarity amino groups (-NH_2) convert to the higher-polarity protonated form (-NH_3^+) in the CM-chitin structure (Schematic 6.1). It is known (Ueno et al. 2007) that polysaccharides such as CM-chitin, which have equatorially-substituted glucopyranose rings, exhibit amphiphilic character, with equatorial hydrophilic edges, and axial hydrophobic planes (see Scheme 6.1), which can strongly interact with the sp^2 hybridized orbital of aromatic rings due to CH-π bonding (Palma *et al.* 2000). Therefore, it appears that the protonated non-cross-linked CM-chitin can act as a weak emulsifying agent, self-assembling with the anilinium ion (protonated aniline) to form a core-shell structure in aqueous solution, where the equatorial hydrophilic groups (including -OH, -NH_3^+, -NH-$COCH_3$, and -OCH_2COOH) orient toward the exterior aqueous phase to form the hydrophilic shell while the axial hydrophobic planes orient towards the interior to form the hydrophobic core. This hydrophobic core may then solubilize the aromatic rings of the aniline molecules, via CH-π bonding, and serve as the reaction template for monomer accumulation (Sahiner 2007). The anilinium ion (protonated aniline) can thus migrate towards the hydrophobic core and form a nucleation site at the interface of the core-shell structure by electrostatic interaction between the chloride anions of the HCl-doped quinoid imine and the ammonium group of the protonated non-cross-linked CM-chitin chains (Jang, Bae, and Lee 2005; Yu *et al.* 2006), as shown in schematic 6.2. With the addition of APS, used as an oxidizing agent, the polymerization of anilinium ions occurs radially from the nucleation site in the template, which provides the local environment to promote the *para*-substitution or head-to-tail coupling of the anilinium ion radical (Cruz-Silva et al. 2005) and hence generate the radially aligned dendritic PANI structure (see Fig. 6.2b). It should be noted that further work needs to be done to establish the details of the proposed templating mechanism via emulsification of the polymerizing aniline by CM-chitin (Schem. 6.2), e.g. whether a single CM-chitin chain or cluster of chains is involved in emulsifying the aniline, or whether each chain forms a single nucleating site or multiple

nucleation sites. Future studies of the effect of molecular weight, degree of deacetylation and degree of carboxylation of the CM-chitin on nanoparticle morphology are planned to yield more insight into the templating mechanism of CM-chitin.

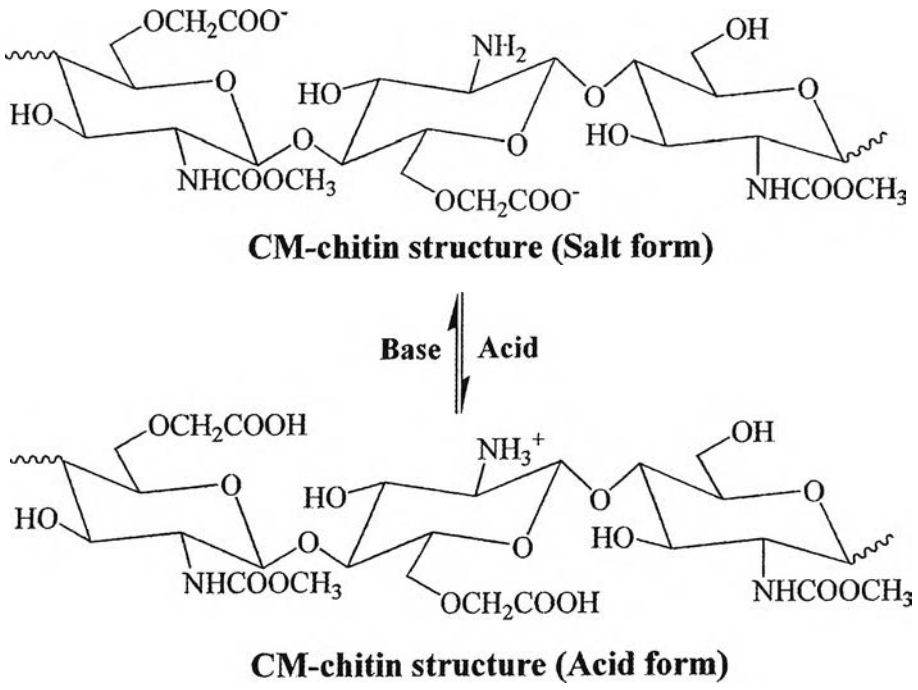

Schematic 6.1 CM-chitin structures under acid-base conditions.

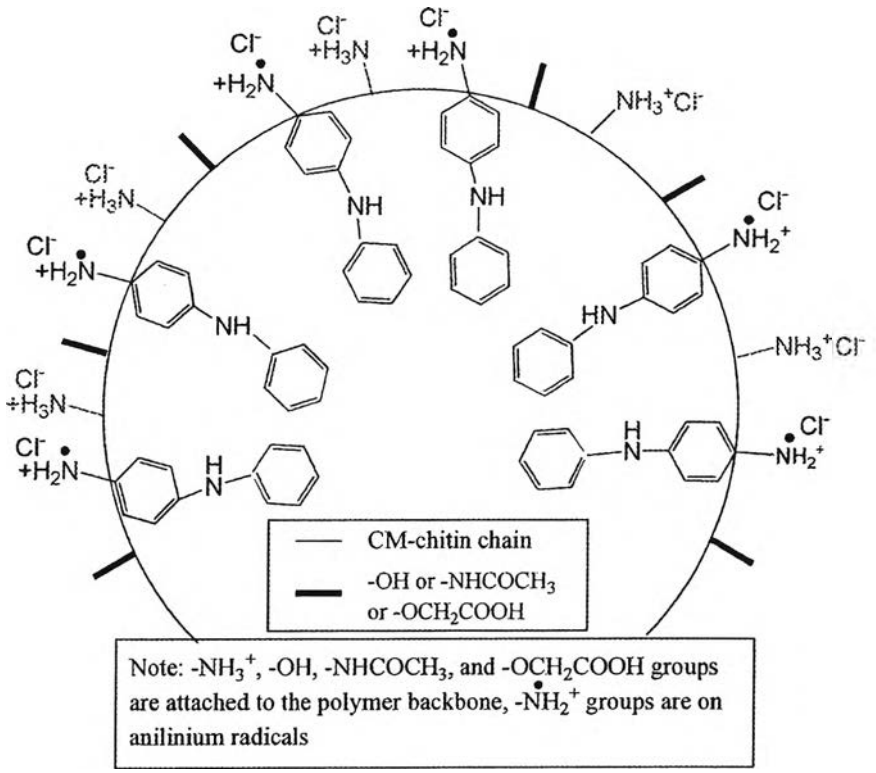

Schematic 6.2 Proposed formation mechanism of synthesized PANI nanoparticles using non-cross-linked CM-chitin template. Note, not shown in the diagram is the associated water of asolvation which accompany the clustering of anilinium ions.

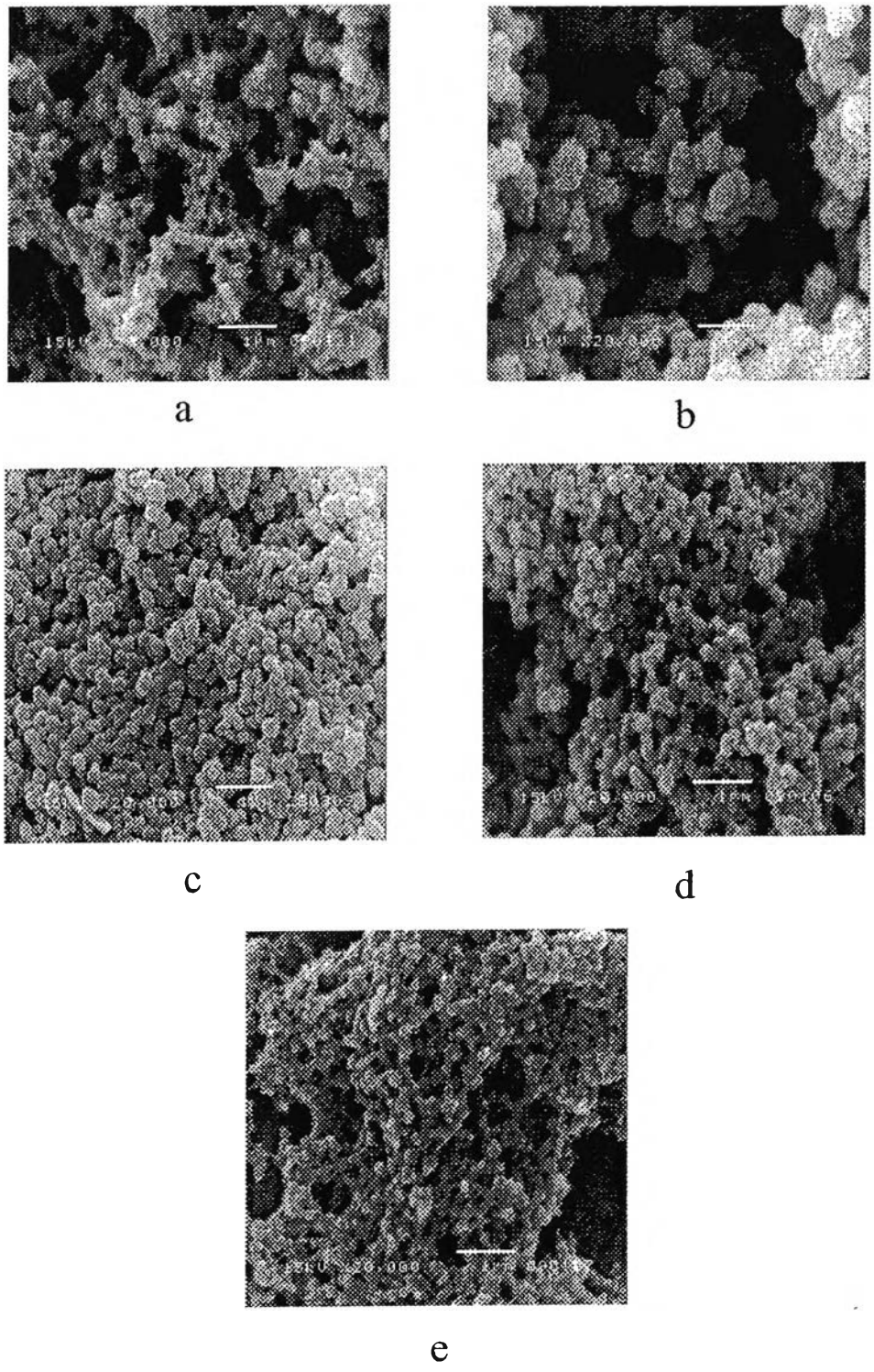

Figure 6.2 SEM images of the synthesized PANI: a) conventional PANI; b) PANI-(1CMCT-0Glu); c) PANI-(1CMCT-3Glu); d) PANI-(1CMCT-9Glu); and, e) PANI-(1CMCT-18Glu).

Importantly, it was found that the size of the synthesized PANI nanoparticles significantly decreased from 392 ± 34 nm to 246 ± 38 nm, and the morphology became more spherical, when the CM-chitin was cross-linked using 3 μmole of glutaraldehyde (1CMCT-3Glu) (Fig. 6.2c). This can be explained by the fact that cross-linking with glutaraldehyde converts the CM-chitin structure to a network structure which restricts the chain mobility and limits the volume of free spaces or pores available to sequester and distribute the aniline monomer (Zhang, Cheng, and Ying 2006). These pores can thus act as nanoreactors, and, as described above for non-crosslinked CM-chitin, the hydrophobic surfaces of the pores may serve as templates for the polymerization of the sequestered anilinium ion in the presence of 1.5 M HCl. On addition of APS, the sequestered anilinium ions subsequently polymerize to fill the individual pores of the cross-linked CM-chitin network structure, as shown in schematic 6.3. Moreover, since only a very small amount of glutaraldehyde (3 μmole) was used to prepare the cross-linked CM-chitin template, the resulting lightly cross-linked CM-chitin template remains soluble in water and can be removed by simply washing with distilled water, to obtain pristine PANI nanoparticles, whose morphology is preserved. Therefore, the utilization of cross-linked CM-chitin as a template for the synthesis of PANI nanoparticles appears to be a simple method to produce tailored PANI nanoparticles with uniform morphology and narrow size distribution.

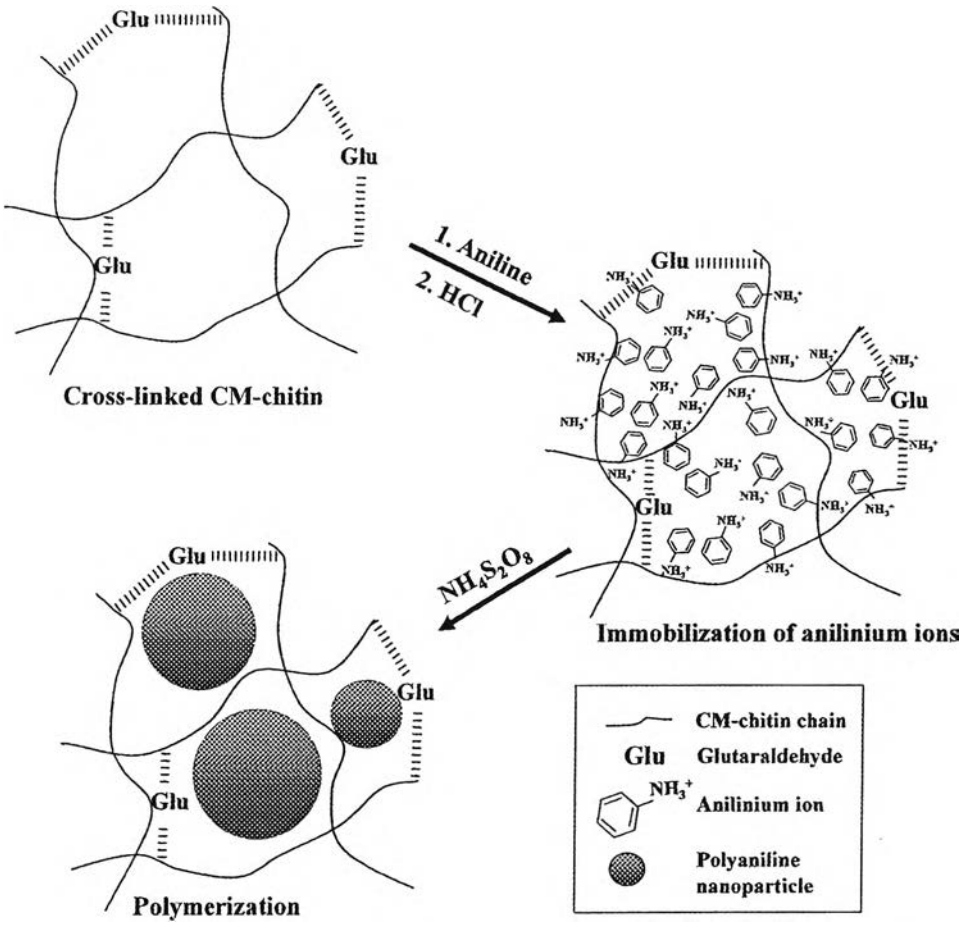

Schematic 6.3 Proposed formation mechanism of synthesized PANI nanoparticles using cross-linked CM-chitin template. Note, not shown in the diagram are the chloride counterions and associated water of asolvation which accompany the clustering of anilinium ions.

In addition, it was found that the size of the PANI nanoparticles can be controlled by varying the degree of cross-linking of the CM-chitin. From figure 6.2, it is seen that the glutaraldehyde concentration used to prepare the cross-linked CM-chitin template determines the size of the resulting PANI nanoparticles (see Fig 6.2b, 6.2c, and 6.2d). Specifically, as the glutaraldehyde concentration increased from 3 μmole (1CMCT-3Glu) to 9 μmole (1CMCT-9Glu), the size of PANI nanoparticles produced in the cross-linked CM-chitin decreased from 246 ± 38 to 160 ± 19 nm, as shown in figure 6.2c and 6.2d, respectively. Thus, a higher degree of cross-linking of CM-chitin (*i.e.* a higher glutaraldehyde concentration) results in formation of

smaller-sized PANI nanoparticles, presumable because of a reduction in size of the pore spaces within the network structure (Mohan *et al.* 2007). However, as seen in Fig. 6.2e, at 18 μmole of glutaraldehyde concentration (1CMCT-18Glu), an aggregated PANI network was obtained. This result may be due, in part, to more limited penetration of aniline monomer inside the pores of the cross-linked CM-chitin so that polymerization occurs both in the inner pores and the outer surfaces of the cross-linked CM-chitin. Moreover, the higher degree of cross-linking (CM-chitin solution containing 18 μmole glutaraldehyde) creates difficulty in template removal due to the stronger intermolecular interaction between the CM-chitin chains. This results in the presence of residual cross-linked CM-chitin in the resulting PANI product, as confirmed by FTIR and TGA results.

6.4.3 FTIR Spectra

FTIR spectra were used to determine the chemical structure of cross-linked CM-chitin (acid form), acting as a template, conventional PANI, and PANI nanoparticles obtained using CM-chitin templates having different degrees of cross-linking, as shown in figure 6.3. The acid form of cross-linked CM-chitin (protonated cross-linked CM-chitin), occurring in the acidic conditions used as the template for the polymerization of aniline, exhibits characteristic peaks at 1743, 1650, 1379, and 1067 cm^{-1} (Fig. 6.3e), attributed, respectively, to COOH stretching, asymmetric C=O, symmetric C=O stretching, and C-O-C stretching of the pyranose ring (Mi et al. 1997). After polymerization of aniline, and removal of the cross-linked CM-chitin by washing with distilled water, the obtained PANI nanoparticles show characteristic peaks at approximately 1565, 1482, 1293, 1100, and 789 cm^{-1}, attributed, respectively, to C=C stretching of the quinoid ring, C=C stretching of the benzenoid ring, C-N stretching, N=Q=N stretching (Q representing the quinoid ring), and out-of-plane C-H stretching in the 1, 4-disubstituted benzene ring (Bai *et al.* 2007; He 2005) as seen in figures 6.3b-6.3c. In addition, these characteristic peaks of the PANI nanoparticles are identical to those we observed for the emeraldine salt form of PANI (PANI ES) synthesized by conventional method (without the addition of CM-chitin template) (Fig. 6.3a). This indicates that the cross-linked CM-chitin template causes only a change in morphology and size of PANI nanoparticles, and does not affect the

chemical structure of the resulting PANI. However, a peak at 1739 cm^{-1}, characteristic of COOH stretching, was observed in the PANI nanoparticles synthesized in the presence of 18 µmole glutaraldehyde-added CM-chitin solutions (PANI-(1CMCT-18Glu)), indicative of residual cross-linked CM-chitin, (Fig. 6.3d). This indicates that too high a degree of cross-linking of CM-chitin chain, results in insolubility in water and incomplete removal of the cross-linked CM-chitin template from the resulting PANI nanoparticles.

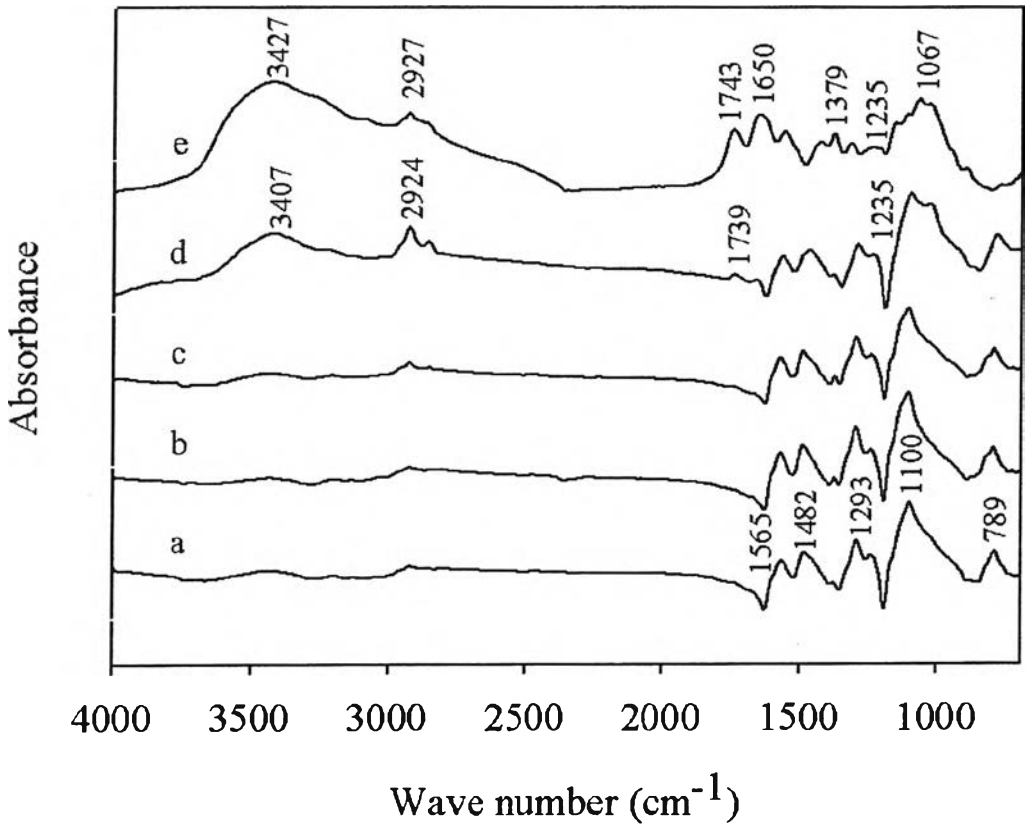

Figure 6.3 FTIR spectra of the synthesized PANI: a) conventional PANI; b) PANI-(1CMCT-3Glu); c) PANI-(1CMCT-9Glu); d) PANI-(1CMCT-18Glu); and, e) cross-linked CM-chitin (acid form).

6.4.4 Thermogravimetric Analysis (TGA)

The thermal properties of cross-linked CM-chitin template, conventional PANI, and PANI nanoparticles synthesized in the presence of CM-

chitin with different glutaraldehyde concentrations is compared in figure 6.4. The PANI nanoparticles synthesized using 3 µmole (PANI-(1CMCT-3Glu)) and 9 µmole (PANI-(1CMCT-9Glu)) of glutaraldehyde concentrations (Fig. 6.4a and 6.4b) exhibit three discrete weight losses at approximately 100, 280, and 500°C, attributed, respectively to the loss of water, the elimination of dopant molecules, and the degradation of PANI chains (Chan *et al.* 1989; Kan *et al.* 2006; Neoh *et al.* 1990). A similar weight loss pattern was observed in the conventional PANI (Fig. 6.4d) and this suggested the complete removal of the CM-chitin template, cross-linked with 3 µmole and 9 µmole of glutaraldehyde concentrations. In contrast, with increase of glutaraldehyde concentration to 18 µmole (Fig. 6.4c), a distinct weight loss at approximately 287°C, corresponding to degradation of cross-linked CM-chitin (Fig. 6.4e), was observed. This supports the IR evidence that the more highly cross-linked CM-chitin can not be completely removed from the resulting PANI nanoparticles.

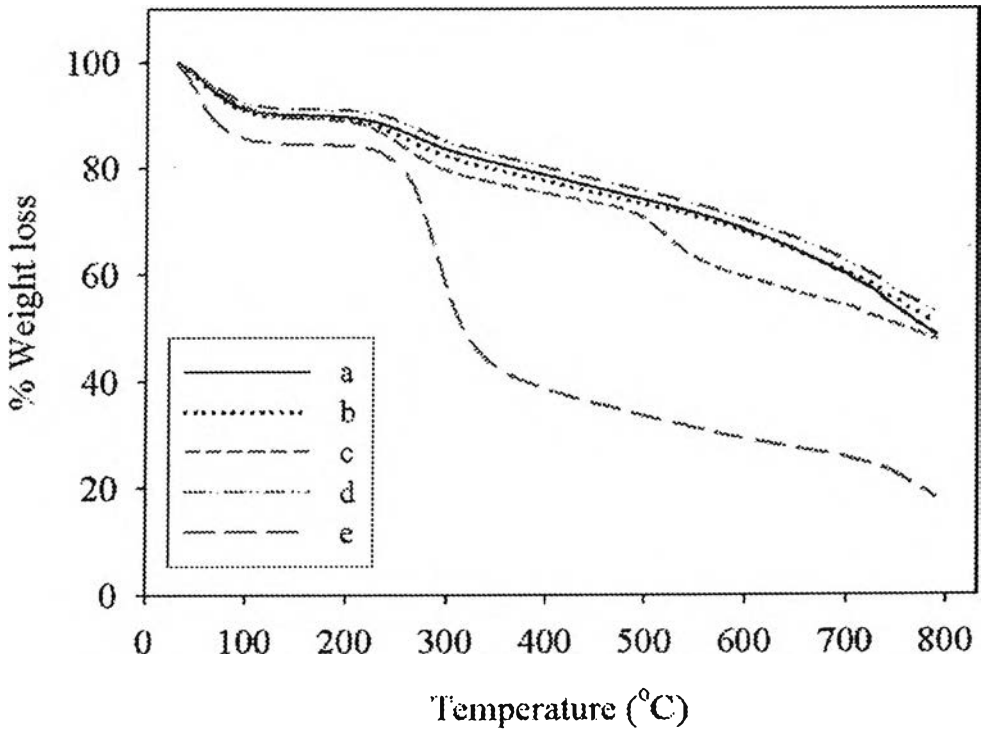

Figure 6.4 TGA thermograms of the synthesized PANI: a) PANI-(1CMCT-3Glu); b) PANI-(1CMCT-9Glu); c) PANI-(1CMCT-18Glu); d) conventional PANI; and, e) cross-linked CM-chitin (acid form).

6.4.5 Wide Angle X-ray Diffraction (WAXD)

Wide angle X-ray diffraction was used to compare the crystal structures of the PANI nanoparticles synthesized in the presence of various glutaraldehyde-containing CM-chitin solutions versus the conventional PANI, as shown in figure 6.5. The pure cross-linked CM-chitin template, shows a weak diffraction peak, $2\theta = 9^{\circ}$, and a broad peak, centered at $2\theta = 20^{\circ}$, which indicates predominantly an amorphous structure (Fig. 6.5d). On the other hand, the conventional PANI exhibits intense diffraction peaks in the range of $2\theta = 9\text{-}30^{\circ}$, as shown in figure 6.5a. This suggests a partially crystalline structure of PANI in the doped state (PANI ES) (Lei and Su 2007; Li, Zhoa *et al.* 2007; Xing *et al.* 2006). The PANI nanoparticles, synthesized using non-cross-linked and cross-linked CM-chitin templates (Fig. 6.5b and 6.5c), show diffraction patterns similar to the conventional PANI, indicating that the use of a non-cross-linked or cross-linked CM-chitin template does not significantly alter the crystal structure of the synthesized PANI products.

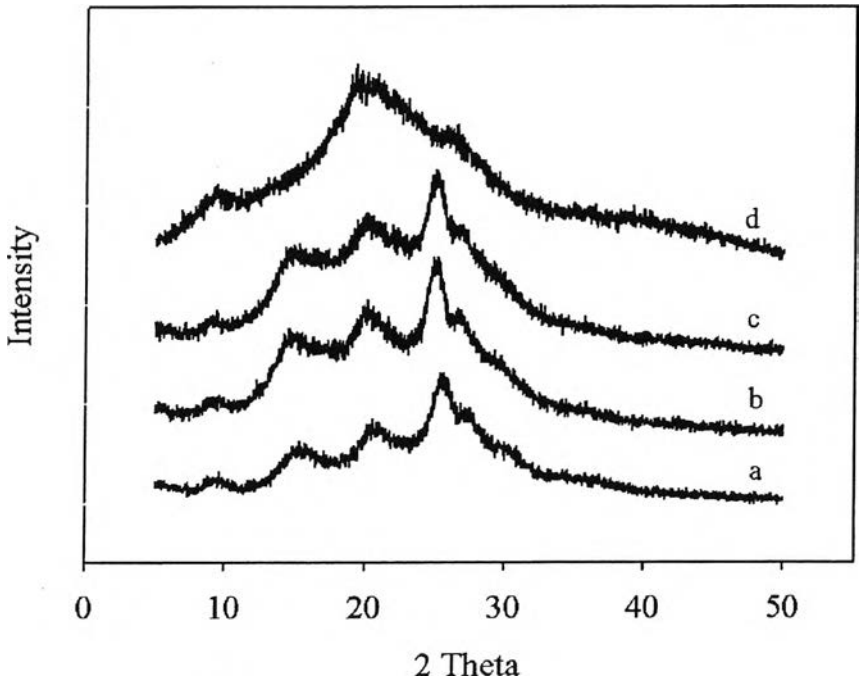

Figure 6.5 XRD patterns of the synthesized PANI: a) conventional PANI; b) PANI-(1CMCT-0Glu); c) PANI-(1CMCT-3Glu); and, d) CM-chitin (acid form).

6.4.6 Electrical Property

The electrical conductivities of the conventional PANI, the PANI nanoparticles synthesized in the presence of non-cross-linked CM-chitin and cross-linked CM-chitin with different glutaraldehyde concentrations, in both undoped (PANI EB) and doped states (PANI ES), are tabulated in table 6.1. It was found that the undoped state of conventional PANI exhibited a conductivity of the order of 10^{-11} S/cm, indicating the insulating form of PANI EB. On the other hand, the electrical conductivity of conventional PANI in the doped state (PANI ES) was higher than that of PANI EB, by approximately 12 orders of magnitude. This is attributed to the highly π-conjugated system and highly ordered structure of PANI ES compared to PANI EB. This is consistent with the XRD evidence of the synthesized PANI products (see figure 6.5). Moreover, we found that the electrical conductivity of PANI ES nanoparticles synthesized in the presence of cross-linked CM-chitin templates is significantly higher than that of conventional PANI ES. This might be due to a higher degree of orientation of the synthesized PANI ES nanoparticles when using the cross-linked CM-chitin template. Nevertheless, a word of caution must be added in that the electrical conductivity was obtained from compressed pellets; that is, the PANI nanoparticles could have undergone morphology changes (when subjected to the pressure of the press) during the sample preparations.

Table 6.1 Electrical conductivity of the PANI nanoparticles in the pellet form

Sample*	Specific conductivity (S/cm)	
	Undoped state**	Doped state
Conventional PANI	$3.72\times10^{-11}\pm 9.86\times10^{-13}$	15.6 ± 0.32
PANI-(1CMCT-0Glu)	$3.99\times10^{-11}\pm 1.52\times10^{-12}$	24.4 ± 1.58
PANI-(1CMCT-3Glu)	$3.52\times10^{-11}\pm 2.36\times10^{-12}$	26.8 ± 2.06
PANI-(1CMCT-9Glu)	$3.07\times10^{-11}\pm 7.97\times10^{-13}$	39.8 ± 2.13
PANI-(1CMCT-18Glu)	$2.01\times10^{-11}\pm 9.80\times10^{-13}$	31.5 ± 0.98

* Sample was prepared by compression of PANI powder.

** The synthesized PANI ES powder was immersed in 1 M NaOH (1 g of PANI ES : 50 g of 1 M NaOH) for 2 h.

6.5 Conclusion

Uniformly globular PANI nanoparticles with a diameter in the nanometer range were successfully synthesized by the oxidative polymerization approach in the presence of a cross-linked CM-chitin template. The molecular structures of the synthesized PANI nanoparticles were identical to those of the conventional PANI. The amount of glutaraldehyde-added CM-chitin was found to play an important role in determining the size of the obtained PANI nanoparticles. By increasing the concentration of the crosslinker, glutaraldehydes, PANI nanoparticles of smaller sizes were obtained. The formation mechanism of the PANI nanoparticles in the cross-linked CM-chitin template is proposed according to the accumulation and the polymerization of the aniline monomer within the pores of the cross-linked CM-chitin network. The electrical conductivities of the compressed PANI nanoparticles was significantly higher than that of the conventional PANI, attributed to a higher orientation of PANI molecules induced by interaction with the cross-linked CM-chitin template. Therefore, the use of cross-linked CM-chitin, with a specific degree of cross-linking, as a template for the synthesis of PANI nanoparticles may be viable approach to obtain bulk quantities of PANI nanoparticles with controlled sizes and narrow size distribution.

6.6 Acknowledgements

The authors gratefully acknowledge Thailand Research Fund (Royal Golden Jubilee Ph.D Scholarship) and The Conductive and Electroactive Polymers Research Unit, Chulalongkorn University, Thailand, for their financial support of this work. We also acknowledge Surapon Food Public Co. Ltd. for supplying the material for this work.

6.7 References

Bai, X. Li, X. Li, N. Zuo, Y. Wang, L. Li, J. and Qiu, S. (2007) Synthesis of cluster polyaniline nanorod via a binary oxidant system. Material Science and Engineering C, 27, 695-699.

Banerjee, P. and Mandal, B.M. (1995) Blends of HCl-doped polyaniline nanoparticles and poly(vinyl chloride) with extremely low percolation threshold -a morphology study. Synthetic Metals, 74, 257-261.

Baxter, A. Dillon, M. and Taylor, K.D.A. (1992) Improved method for i.r. determination of the degree of N-acetylation of chitosan. International Journal of Biological Macromolecules, 14, 166-169.

Cao, Y. Smith, P. and Heeger, A.J. (1992) Counter-ion induced processibility of conducting polyaniline and of conducting polyblends of polyaniline in bulk polymers. Synthetic Metals, 48, 91-97.

Chan, H.S.O. Teo, M.T.B. Khor, E. and Lim, C.N. (1989) Thermal analysis of conducting polymers part I thermogravimetry of acid-doped polyanilines. Journal Thermal Analysis and Calorimetry, 35, 765–774.

Cheng, C. Jiang, J. Tang, R. and Xi, F. (2004) Polyaniline nanostructures doped with mono-sulfonated dendrons via a self-assembly process. Synthetic Metals, 145, 61-65.

Cheng, D. Ng, S. and Chan, H.S.O. (2005) Morphology of polyaniline nanoparticles synthesized in triblock copolymers micelles. Thin Film Solid, 477, 19-23.

Chiou, N.R. and Epstein, A.J. (2005) A Simple Approach to Control the Growth of Polyaniline Nanofibers. Synthetic Metals, 153, 69-72.

Cho, M.S. Park, S.Y. Hwang, J.Y. and Choi, H.J. (2004) Synthesis and electrical properties of polymer composites with polyaniline nanoparticles. Material Science and Engineering C, 24, 15-18.

Cruz-Silva, R. Romero-Garcia, J. Angulo-Sanchez, J.L. Ledezma-Perez, A. Arias-Matin, E. Moggio, I. and Flore-Loyola, E (2005) Template-free enzymatic synthesis of electrically conducting polyaniline using soybean peroxidase. European Polymer Journal, 41, 1129-1135.

Gu, D.W. Li, J.S. Li, J.L. Cai, Y.M. and Shen, L.J. (2005) Polyaniline thin films in situ polymerized under very high pressure. Synthetic Metals, 150, 175–179.

He, H.X. Li, C.Z. and Tao, N.J. (2001) Conductance of polymer nanowires fabricated by a combined electrodeposition and mechanical break junction method. Applied Physics Letters, 78, 811-813.

He, Y. (2005) Interfacial synthesis and characterization of polyaniline nanofibers. Material Science and Engineering B, 122, 76-79.

He, Y. (2005) Preparation of polyaniline microspheres with nanostructured surfaces by a solids-stabilized emulsion. Material Letters, 59, 2133-2136.

Hopkins, A.R. Lipeles, R.A. and Kao, W.H. (2004) Electrically conducting polyaniline microtube blends. Thin Solid Film, 447-448, 474-480.

Huang, J. and Kaner, R.B. (2004) A general chemical route to polyaniline nanofibers. Journal of the American Chemical Society, 126, 851-855.

Huang, J. Virji, S. Weiller, B.H. and Kaner, R.B. (2004) Nanostructured polyaniline sensors. Chemical - A European Journal, 10, 1314-1319.

Jang, J. Bae, J, and Lee, K. (2005) Synthesis and characterization of polyaniline nanorods as curing agent and nanofiller for epoxy matrix composite. Polymer, 46, 3677-3684.

Jing, X. Wang, Y. Wu, D. and Qiang, J. (2007) Sonochemical synthesis of polyaniline nanofibers. Ultrasonics Sonochemistry, 14, 75-80.

Jing, X. Wang, Y. Wu, D. She, L. and Guo, Y. (2006) Polyaniline nanofibers prepared with ultrasonic irradiation. Journal of Polymer Science Part A: Polymer Chemistry, 44, 1014-1019.

Kan, J. Zhou, S. Zhang, Y. and Patel, M. (2006) Synthesis and characterization of polyaniline nanoparticles in the presence of

magnetic field and samarium chloride. European Polymer Journal, 42, 2004-2012.

Lei, X. and Su, Z. (2007) Novel conducting polyaniline copolymers of aniline and N-phenylglycine. Material Letters, 61, 1158-1161.

Li, M. Gou, Y. Wei, Y. MacDiarmid, A.G. Lelkes, P.I. (2006) Electrospinning polyaniline-contained gelatin nanofibers for tissue engineering applications. Biomaterials, 27, 2705-2715.

Li, X. Zhoa, Y. Zhuang, T. Wang, G. and Gu, Q. (2007) Self-dispersible conducting polyaniline nanofibres synthesized in the presence of β-cyclodextrin. Colloids and Surfaces A, 295, 146-151.

Liu, H.Q. and Kaner, R.B. (2004) A general chemical route to polyaniline nanofibers. Journal of the American Chemical Society 126, 851-855.

Lu, X. Yu, Y. Chen, L. Mao, H. Wang, L. Zhang, W. and Wei, Y. (2005) Poly(acrylic acid)-guided synthesis of helical polyaniline microwires. Polymer, 46, 5329-5333.

Martin, C.R. (1996) Membrane-based synthesis of nanomaterials. Chemistry of Materials, 8, 1739-1746.

Mazur, M. Tagowska, M. Palys, B. and Jakowska, K. (2003) Template synthesis of polyaniline and poly(2-methoxyaniline) nanotubes: comparison of the formation mechanisms. Electro - chemistry Communications, 5, 403-407.

Mi, F.L. Chen, C.T. Tseng, Y.C. Kuan, C.Y. and Shyu, S.S. (1997) Iron(III)-carboxymethylchitin microsphere for the pH-sensitive release of 6-mercaptopurine. Journal of Controlled Release, 44, 19-32.

Mohan, Y.M. Lee, K. Premkumar, T. Geckeler, K.E. (2007) Hydrogel networks as nanoreactors: a novel approach to silver nanoparticles for antibacterial applications. Polymer, 48, 158-164.

Neoh, K.G. Kang, E.T. and Tan, K.L. (1990) Thermal degradation of leucoemeraldine, emeraldine base and their complexes. Thermochimica Acta. 171, 279–291.

Palma, R. Himmel, M.E. and Brady, J.W. (2000) Calculation of the Potential of Mean Force for the Binding of Glucose to Benzene in Aqueous Solution. Journal of Physical ChemistryB, 104, 7228–7234.

Sahiner, N. (2007) Hydrogel nanonetworks with functional core–shell structure. European Polymer Journal, 43, 1709-1717.

Stejskal, J. Sapurina, I. Trchova, M. Konyushenko, E.N. and Holler, P. (2006) The genesis of polyaniline nanotubes. Polymer, 47, 8253-8262.

Strachotova, B. Strachota, A. Uchman, M. Brus, S.J. Plestil, J. and Matejka, L. (2007) Super porous organic–inorganic poly(N-isopropylacrylamide)-based hydrogel with a very fast temperature response. Polymer, 48, 1471-1482.

Thanpitcha, T. Sirivat, S. Jamieson, A.M. and Rujiravanit, R. (2006) Preparation and characterization of polyaniline/chitosan blend film. Carbohydrate Polymer, 64, 560-568.

Ueno, T. Yokota, S. Kitaoka, T. Wariishi, H. (2007) Conformational changes in single carboxymethylcellulose chains on a highly oriented pyrolytic graphite surface under different salt conditions. Carbohydrate Research, 342, 954-960.

Virji, S. Huang, J. Kaner, R.B. Weiller, B.H. (2004) Polyaniline nanofiber gas sensors: examination of response mechanisms. Nano Letters, 4, 491-496.

Wang, Y. and Jing, X. (2005) Radiolytic synthesis of polyaniline nanofibers: a new templateless pathway. Chemistry of Materials, 17, 227-229.

Wang, Y. Jing, X. and Kong, J. (2007) Polyaniline nanofibers prepared with hydrogen peroxide as oxidant. Synthetic Metals, 157, 269-275.

Wang, Y. and Jing, X. (2008) Formation of polyaniline nanofibers: a morphological study. Journal of Physical Chemistry B, 112, 1157-1162.

Wang, Z. Chen, M. and Li, H. (2002) Preparation and characterization of uniform polyaniline nano-fibrils using the anodic aluminum oxide template. Material Science and Engineering A, 328, 33-38.

Wei, D. Kvarnstrom, C. Lindfors, T. and Ivaska, A. (2006) Polyaniline nanotubules obtained in room-temperature ionic liquids. Electro-chemistry Communications, 8, 1563-1566.

Werake, L.K. Story, J.G. Bertino, M.F. Pillalamarri, S.K. and Blum, F.D. (2005) Photolithographic synthesis of polyaniline nanofibres. Nanotechnology, 16, 2833-2837.

Wongpanit, P. Sanchavanakit, N. Pavasant, P. Supaphol, P. Tokura, S. and Rujiravanit, R. (2005) Preparation and Characterization of Microwave-treated Carboxymethyl Chitin and Carboxymethyl Chitosan Films for Potential Use in Wound Care Application. Macromolecular Bioscience, 5, 1001-1012.

Wu, C.G. and Bein, T. (1994). Conducting polyaniline filaments in a mesoporous channel host. Science, 264, 1757-1759.

Xian, Y. Liu, F. Feng, L. Wu, F. Wang, L. and Jin, L. (2007) Nanoelectrode ensembles based on conductive polyaniline/poly(acrylic acid) using porous sol–gel films as template. Electro-chemistry Communications, 9: 773-780.

Xing, S. Zhao, C. Jing, S. Wu, Y. and Wang, Z. (2006) Morphology and gas-sensing behavior of in situ polymerized nanostructured polyaniline films. European Polymer Journal, 42, 2730-2735.

Xiong, S. Wang, Q. and Xia, H. (2004) Preparation of polyaniline nanotubes array based on anodic aluminum oxide template. Material Research Bulletin, 39, 1569-1580.

Xiong, S. Wang, Q. and Xia, H. (2004) Template synthesis of polyaniline/TiO_2 bilayer microtubes. Synthetic Metals, 146, 37-42.

Yang, C. Chih, Y. Cheng, H. and Chen, C. (2005) Nanofibers of self-doped polyaniline. Polymer, 46, 10688-10698.

Yu, Y. Zhihuai, S. Chen, S. Bian, C. Chen, W. and Xue, G. (2006) Facile synthesis of polyaniline-sodium alginate nanofibers. Langmuir, 22, 3899-3905.

Zhang, D, and Wang, Y. (2006) Synthesis and applications of one-dimensional nano-structured polyaniline: an overview. Material Science Engineering B, 134, 9-19.

Zhang, F. Cheng, G. and Ying, G. (2006) Emulsion and macromolecules templated alginate based polymer microspheres. Reactive and Functional Polymer, 66, 712-719.

Zhang, X. Goux, W.J. and Manohar, S.K. (2004) Synthesis of polyaniline nanofibers by nanofiber seeding. Journal of the American Chemical Society, 126: 4502-4503.

Zhang, Z. and Wan, M. (2002) Composite films of nanostructured polyaniline with poly(vinyl alcohol). Synthetic Metals, 128, 83-89.

Zhu, J. and Jiang, W. (2007) Fabrication of conductive metallized nanostructures from self-assembled amphiphilic triblock copolymer templates: Nanospheres, nanowires, nanorings. Material Chemistry and Physics, 101, 56-62.